Heliyon 10 (2024) e38647

Contents lists available at ScienceDirect

Heliyon

journal homepage: www.cell.com/heliyon

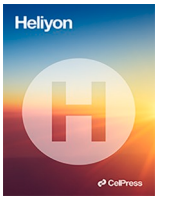

Research article

Cabozantinib prevents the progression of metabolic dysfunction-associated steatohepatitis by inhibiting the activation of hepatic stellate cell and macrophage and attenuating angiogenic activity

Takuya Matsuda, Kosuke Kaji *, Norihisa Nishimura, Shohei Asada, Aritoshi Koizumi, Misako Tanaka, Nobuyuki Yorioka, Yuki Tsuji, Koh Kitagawa, Shinya Sato, Tadashi Namisaki, Takemi Akahane, Hitoshi Yoshiji

Department of Gastroenterology, Nara Medical University, Kashihara, Nara, 634-8521, Japan

ARTICLE INFO

Keywords:
Angiogenesis
Liver fibrosis
MASH
Inflammation
Hepatocarcinogenesis

ABSTRACT

Cabozantinib, a multiple tyrosine kinase inhibitor targeting AXL, vascular endothelial growth factor receptor (VEGFR), and MET, is used clinically to treat certain cancers, including hepatocellular carcinoma. This study aimed to assess the impact of cabozantinib on liver fibrosis and hepatocarcinogenesis in a rat model of metabolic dysfunction-associated steatohepatitis (MASH). MASH-based liver fibrosis and hepatocarcinogenesis were induced in rats by feeding them a choline-deficient, L-amino acid-defined, high-fat diet (CDAHFD) for eight and 16 weeks, respectively. Cabozantinib (1 or 2 mg/kg, daily) was administered concurrently with the diet in the fibrosis model and after eight weeks in the carcinogenesis model. Treatment with cabozantinib significantly attenuated hepatic inflammation and fibrosis without affecting hepatocyte steatosis and ballooning in CDAHFD-fed rats. Cabozantinib-treated rats exhibited a marked reduction in α-smooth muscle actin^{+} activated hepatic stellate cell (HSC) expansion, CD68^{+} macrophage infiltration, and CD34^{+} pathological angiogenesis, along with reduced hepatic AXL, VEGF, and VEGFR2 expression. Consistently, cabozantinib downregulated the hepatic expression of profibrogenic markers (*Acta2*, *Col1a1*, *Tgfb1*), inflammatory cytokines (*Tnfa*, *Il1b*, *Il6*), and proangiogenic markers (*Vegfa*, *Vwf*, *Ang2*). In a cell-based assay of human activated HSCs, cabozantinib inhibited Akt activation induced by GAS6, a ligand of AXL, leading to reduced cell proliferation and profibrogenic activity. Cabozantinib also suppressed lipopolysaccharide-induced proinflammatory responses in human macrophages, VEGFA-induced collagen expression and proliferation in activated HSCs, and VEGFA-stimulated proliferation in vascular endothelial cells. Meanwhile, administration of cabozantinib did not affect Ki67^{+} hepatocyte proliferation or serum albumin levels, indicating no negative impact on regenerative capacity. Treatment with cabozantinib also reduced the placental glutathione transferase^{+} preneoplastic lesions in CDAHFD-fed rats. In conclusion, cabozantinib shows promise as a novel option for preventing MASH progression.

* Corresponding author. Department of Gastroenterology, Nara Medical University, Japan 840 Shijo-cho, Kashihara, Nara, 634-8521, Japan.
E-mail address: kajik@naramed-u.ac.jp (K. Kaji).

https://doi.org/10.1016/j.heliyon.2024.e38647
Received 16 April 2024; Received in revised form 5 September 2024; Accepted 26 September 2024
Available online 27 September 2024

1. Introduction

Metabolic dysfunction-associated steatohepatitis (MASH), formerly recognized as nonalcoholic steatohepatitis, has emerged as a major chronic liver disease worldwide [1–3]. MASH encompasses a spectrum of liver conditions characterized by hepatic steatosis, ballooning, inflammation, and fibrosis. If left untreated, it can progress to cirrhosis and hepatocellular carcinoma (HCC) [4]. Notably, advanced fibrosis is a crucial factor associated with overall mortality, liver transplantation, and liver-related events in patients with MASH [5,6]. Therefore, establishing therapies to manage liver fibrosis is a key challenge in MASH. A recent Phase III trial has shown promising results for resmetirom, a thyroid hormone receptor beta-selective agonist, in improving liver fibrosis in patients with MASH [7]. However, it will take some time for this drug to be available worldwide.

AXL, a receptor tyrosine kinase, is a part of the TAM (TYRO3, AXL, and MERTK) family of receptors [8,9]. It is activated by binding to the ligand growth arrest-specific 6 (GAS6) and plays key roles in immune response modulation, cancer progression, inflammation, and fibrosis [8,10,11]. The GAS6/AXL signaling pathway has been implicated in the pathophysiology of liver diseases. GAS6 exhibits hepatoprotective effects in ischemia/reperfusion-induced injury and is involved in the wound healing response [12–14]. In the injured liver, GAS6 and AXL are primarily expressed in macrophages, including Kupffer cells, and in activated hepatic stellate cells (HSCs) [15]. The GAS6/AXL pathway promotes HSC activation and liver fibrosis in carbon tetrachloride-treated mice [16]. In patients, serum levels of GAS6 and soluble AXL increase during the progression of chronic liver diseases, including alcoholic liver disease and chronic hepatitis C [16]. Additionally, Tutusaus et al. have revealed elevated levels of GAS6 and soluble AXL in patients with MASH [11]. They also demonstrated that bemcentinib, a AXL inhibitor, prevented liver injury in a diet-induced MASH model, with the preventive effect limited to the early stage of MASH [11]. Pathological angiogenesis has been reported to be closely linked to fibrogenesis in the progression of chronic liver disease [17]. Vascular endothelial growth factor-A (VEGFA), a proangiogenic factor, has been reported to play a profibrogenic role *via* multiple mechanisms, including the release of inflammatory and fibbrogenic mediators from endothelial cells, and directly affecting HSCs [17–19]. These functional mechanisms suggest that inhibiting the VEGFA/VEGFR pathway has potential benefits for resolving fibrosis. Indeed, early studies have suggested that targeting VEGFR with tyrosine kinase inhibitors (TKIs) can prevent liver fibrosis progression and reduce intrahepatic angiogenesis [20,21]. Additionally, recent research has demonstrated that hepatocytes produce VEGFA, which activates adjacent HSCs and accelerates the MASH-HCC transition [22].

Cabozantinib, an orally administered small-molecule TKI, primarily targets VEGFR1-3, AXL, and c-MET [23]. In the clinical phase III trial conducted in 2018, cabozantinib demonstrated clinical efficacy as a second- or third-line treatment for unresectable HCC [24]. However, the impact of cabozantinib's inhibitory effects on AXL and VEGFR and, subsequently, liver fibrosis development and hepatocarcinogenesis is still obscure in MASH.

The aim of this study was to determine the effects of cabozantinib on liver fibrosis progression and hepatocarcinogenesis in a diet-induced MASH rat model.

2. Materials and methods

2.1. Animals and reagents

Six-week-old male F344/NSlc rats (Japan SLC, Hamamatsu, Japan) were housed in stainless steel mesh cages under controlled conditions (temperature: 23 °C ± 3 °C, relative humidity: 50 % ± 20 %, ventilation: 10–15 times/h, illumination: 12 h/day). During the study period, rats were allowed to drink tap water freely. This study was reviewed and approved by the Ethics Committee of Nara Medical University and conducted in accordance with the Guide for the Care and Use of Laboratory Animals of the U.S. National Research Council (approval no. 13119). Cabozantinib was purchased from Chemscene (Monmouth Junction, NJ, USA).

2.2. Animal experiments

Rats were fed a choline-deficient, L-amino acid-defined, high-fat diet (CDAHFD) to develop MASH liver fibrosis for eight weeks and liver carcinogenesis for 16 weeks. A choline-supplemented L-amino acid-defined, normal-fat diet (CSANFD) was used as a negative control. The ingredient compositions of both diets were shown in Supplementary Material (Supplementary Table 1) (Research Diets Inc., New Brunswick, NJ, USA). For the fibrosis model, rats were grouped as follows ($n = 8$): (i) fed with CSANFD and administered vehicle (CS), (ii–iv) fed with CDAHFD and administered (ii) vehicle (CD + Veh), (iii) cabozantinib (1 mg/kg/day; CD + CBZ-L), and (iv) cabozantinib (2 mg/kg/day; CD + CBZ-H). Saline was used as the vehicle, and administration of the vehicle and cabozantinib was initiated with the feeding of CSANFD or CDAHFD by gavage daily throughout the study. For the carcinogenesis model, rats were also grouped ($n = 8$), as in the fibrosis model, with cabozantinib administered eight weeks after starting the CSANFD or CDAHFD diet. After the experimental period, blood was collected, serum was separated, and animals were killed using mild isoflurane anesthesia. The whole liver samples were retrieved for biochemical, histopathological and molecular analysis.

2.3. Biochemical analysis

Serum aspartate aminotransferase, alanine aminotransferase, and albumin levels were determined by enzyme-linked immunosorbent assay (ELISA) kits (Abcam, Cambridge, UK) and Rat GAS6 Sandwich ELISA Kit (LSBio, Seattle, WA, USA) was used to measure serum GAS6 levels. ELISA assays were performed according to the accompanying instructions.

2.4. Histological analysis

Liver samples were fixed in 4 % paraformaldehyde and processed into paraffin sections for hematoxylin and eosin (H&E) and Sirius Red staining. The pathological score was independently determined by two pathologists to assess liver tissue steatosis, ballooning, and inflammation, as described previously [25]. Immunohistochemical staining was performed as previously described [21]. The primary antibodies include a rabbit monoclonal α-smooth muscle actin (ab124964, 1:1000, Abcam), a mouse monoclonal CD68 (GTX41868, 1:50, GeneTex, Irvine, CA, USA), a rabbit monoclonal CD34 (ab81289, 1:2500, Abcam), and a rabbit polyclonal antibody against placental glutathione transferase (GST-P; 311, 1:300, Medical and Biological Laboratories, Nagoya, Japan). Immunofluorescence analysis was performed to evaluate hepatocyte expression and cell proliferation, respectively, as previously described [21]. The primary antibodies used were a rabbit monoclonal glutamine synthetase (GS) (ab176562, 1:500, Abcam) and a mouse monoclonal Ki67 (NBP2-22112, 1:100, Novus Biologicals, Centennial, CO, USA). Semiquantitative analysis was performed as described [21].

2.5. Hepatic hydroxyproline content

The hepatic hydroxyproline content was measured in frozen rat liver tissue using the Hydroxyproline Assay Kit (Cell Biolabs, Inc., San Diego, CA, USA) according to the manufacturer's instructions.

2.6. Cell culture and treatment

Human activated HSCs (LX-2, Cat: SCC064, Merck KGaA, Darmstadt, Germany) and human umbilical vein endothelial cells (HUEhT-1, RRID: CVCL_4W51, the National Institutes of Biomedical Innovation, Health, and Nutrition, Osaka, Japan) were cultured in Dulbecco's Modified Eagle's Medium (Nacalai Tesque Inc., Kyoto, Japan), while human monocyte-macrophages (THP-1, RRID: CVCL_0006, the National Institutes of Biomedical Innovation, Health, and Nutrition) were cultured in Roswell Park Memorial Institute 1640 medium (Nakalai Tesque Inc.). The cells were incubated at 37 °C in a 5 % CO_2 in each medium supplemented with 5 % fetal bovine serum (Gibco, Waltham, MA, USA) and 1 % penicillin and streptomycin. LX-2 cells were treated with recombinant human GAS6 (rGAS6; 500 ng/mL; R&D Systems) or recombinant human VEGF 165 (VEGFA; 10 ng/mL; Peprotech, Waltham, MA, USA) to stimulate cell proliferation and profibrogenic activity. THP-1 cells were treated with the lipopolysaccharide *Escherichia coli* 0111:B4 (LPS; 50 ng/mL; Sigma-Aldrich, St. Louis, MO, USA) for 24 h to induce an inflammatory response. HUEhT-1 cells were stimulated with VEGFA (10 ng/mL) to induce proliferation.

2.7. Cell viability and proliferation assays

LX-2, THP-1 and HUEhT-1 cells were seeded in 96-well plates with DMEM which included 10 % FBS for 24 h. After the exposure to cabozantinib (0–500 nM) for 24 h, cell viability was determined by the Premix WST-1 Cell Proliferation Assay system (Takara Bio, Shiga, Japan). Meanwhile, LX-2 cells were pretreated with rGAS6 (500 ng/mL) or VEGFA (10 ng/mL), and HUEhT-1 cells were pretreated with VEGFA (10 ng/mL). After a 6-h pretreatment, cabozantinib (0, 1, 10, and 50 nM) were added. Cell proliferation was then assessed after 24, 48, and 72 h by the BrdU Cell Proliferation ELISA Kit (Cosmo Bio, Tokyo, Japan).

2.8. RNA extraction and real-time polymerase chain reaction (RT-qPCR)

Total RNA was extracted from both cultured cells and rat liver tissue tissues using QIAzole and Qiagen RNeasy Mini Kits (Qiagen, Hilden, Germany). Following the assessment of RNA purity and concentration, reverse transcription to complementary DNA was carried out using the SYBR Green master mix (Applied Biosystems, Waltham, MA, USA). Quantitative RT-PCR was performed employing the StepOnePlus™ Real-Time PCR system (Applied Biosystems). Glyceraldehyde 3-phosphate dehydrogenase (GAPDH) served as the reference gene. The determination of relative mRNA expression levels was achieved using the $2^{-\Delta\Delta Ct}$ method. Detailed primer sequences can be found in Supplementary Material (Supplementary Table 2).

2.9. Protein extraction and western blotting

LX-2 cells were lysed using Mammalian Protein Extraction Reagent (Thermo Fisher Scientific) and mixed with Halt™ Protease and Phosphatase Inhibitor Cocktail (Thermo Fisher Scientific) from 1×10^6 cultured cells. 20 μg proteins were added to each lane for SDS-PAGE gel electrophoresis, and then the protein bands were transferred to Invitrolon™ Polyvinylidene Difluoride membrane (Thermo Fisher Scientific). The membrane was then sealed with 5 % skim milk at room temperature for 1 h. After Tris-buffered saline containing 0.1 % Tween-20 (TBST) cleaning, the primary antibody was added and incubated overnight at 4 °C. The primary antibodies include rabbit Phospho-AXL (Tyr702; #5724; 1:1000), rabbit AXL (#8661; 1:1000), rabbit Phospho-Akt (Ser473; #9271; 1:1000), and rabbit Akt (#9272; 1:1000), all obtained from Cell Signaling Technology, Danvers, MA, USA. After another round of TBST cleaning, the secondary antibody was added and incubated at room temperature for 1 h. Finally, chemiluminescence was used to detect the target bands.

2.10. Statistical analyses

Statistical analyses were performed using GraphPad Prism 9 (version 9.0.0, GraphPad Software, Inc., USA). All results were presented as the means and standard deviations of at least three independent experiments. All data are expressed as mean ± standard deviation. Independent *t*-test was used to compare two independent samples. The difference was statistically significant for $p < 0.05$.

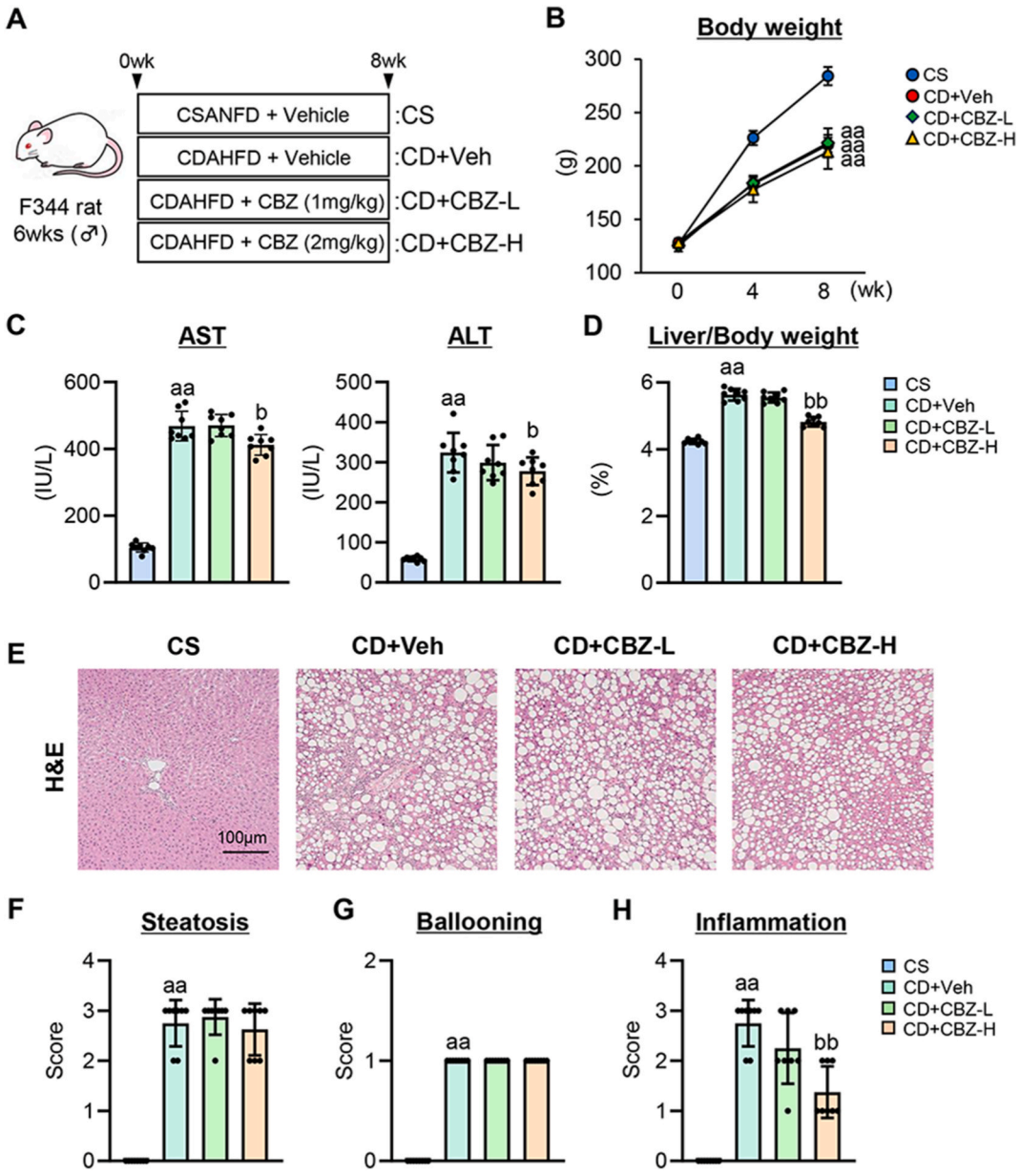

Fig. 1. Effect of cabozantinib on hepatic inflammation in CDAHFD-fed rats. (A) Experimental design of CDAHFD-induced liver fibrosis. (B) Changes in the body weights during the experimental period. (C) Serum levels of aspartate aminotransferase (AST) and alanine aminotransferase (ALT). (D) Liver/body weight at the end of experiment. (E) Representative microphotographs of hematoxylin and eosin (H&E) of the livers in the experimental rats. (F–H) Pathological scores for (F) steatosis, (G) ballooning and (H) inflammation at a 400-fold magnification. Data are the mean ± SD (n = 8; B–D, F–H). [a, aa]: $P < 0.05$, 0.01 vs CS group, [b, bb]: $P < 0.05$, 0.01 vs CD + Veh group, significant difference between groups by Student's t-test. CS, CSANFD-fed and vehicle-treated group; CD + Veh, CDAHFD-fed and vehicle-treated group; CD + CBZ-L, CDAHFD-fed and cabozantinib (1 mg/kg)-treated group; CD + CBZ-H, CDAHFD-fed and cabozantinib (2 mg/kg)-treated group.

3. Results

3.1. Cabozantinib suppresses hepatic inflammation in CDAHFD-fed rats

Fig. 1A illustrates the experimental design for MASH liver fibrosis. Rats were fed CDAHFD for eight weeks, resulting in a significant delay in body weight gain (Fig. 1B) (26). Administration of cabozantinib did not affect the CDAHFD-induced weight loss at doses of 1 and 2 mg/kg (Fig. 1B). Oral intake remained unchanged with cabozantinib administration (data not shown). CDAHFD-fed rats showed a marked increase in serum levels of hepatic enzymes, which were reduced by cabozantinib treatment at 2 mg/kg (Fig. 1C). Significant hepatomegaly was observed in CDAHFD-fed rats, while treatment with cabozantinib (2 mg/kg) attenuated this effect (Fig. 1D). Histological analysis with H&E staining revealed reduced hepatic inflammation in cabozantinib-treated CDAHFD-fed rats, whereas hepatocytic steatosis and ballooning were not affected (Fig. 1E–1H).

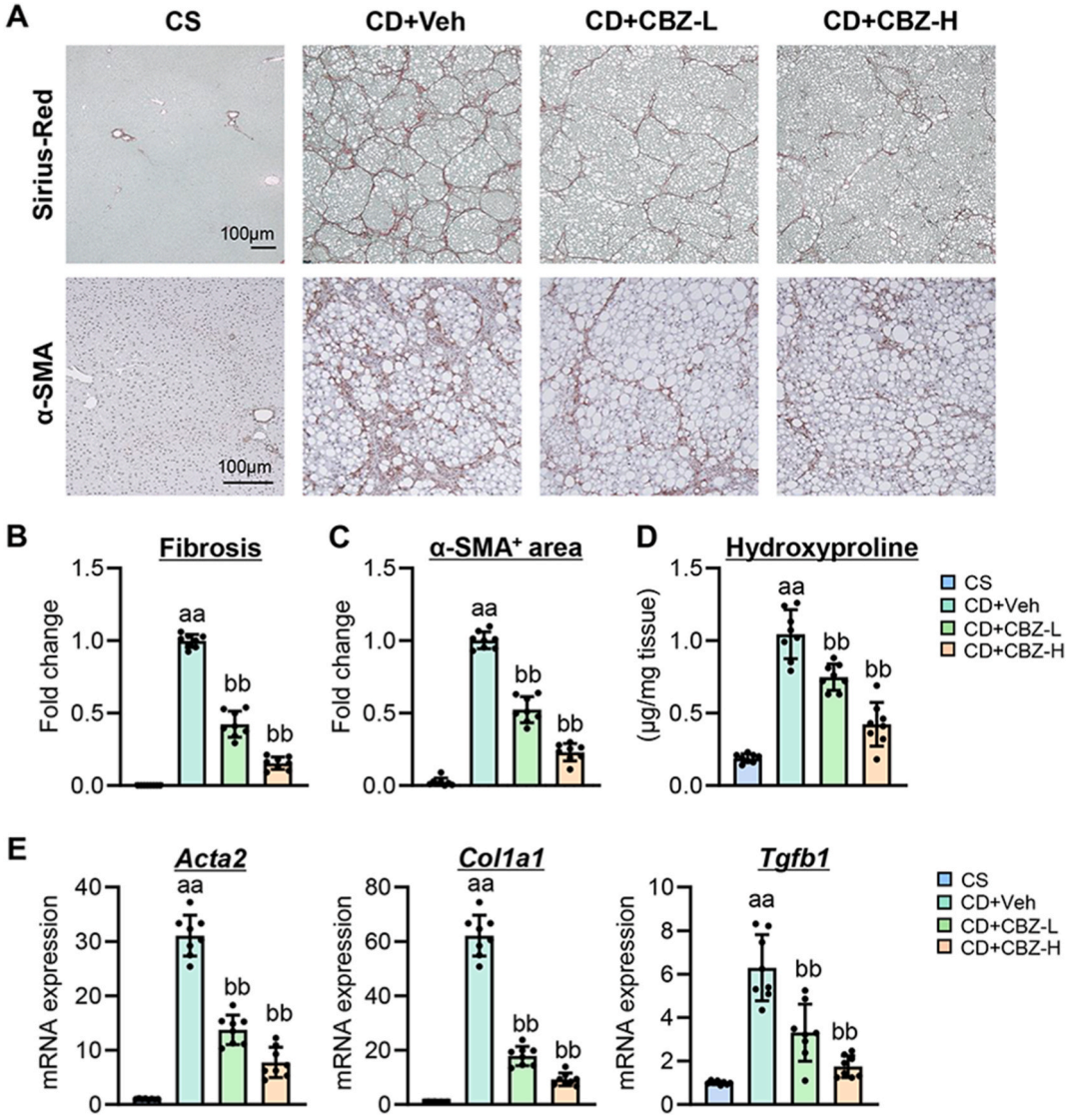

Fig. 2. Effect of cabozantinib on hepatic fibrosis in CDAHFD-fed rats. (A) Representative microphotographs of Sirius-Red and α-smooth muscle actin (SMA) staining of the livers in the experimental rats. (B and C) Quantification of (B) Sirius-Red stained fibrotic area and (C) α-SMA-positive area in high-power field. (D) Hepatic concentration of hydroxyproline. (E) Hepatic mRNA level of profibrotic markers (Acta2, Col1a1 and Tgfb1). Gapdh was used as an internal control for qRT-PCR. Quantitative values are indicated as fold changes to the values of CD + Veh group (B and C) or CS group (E). Data are the mean ± SD (n = 8; B–E). $^{a, aa}$: $P < 0.05$, 0.01 vs CS group, $^{b, bb}$: $P < 0.05$, 0.01 vs CD + Veh group, significant difference between groups by Student's t-test. CS, CSANFD-fed and vehicle-treated group; CD + Veh, CDAHFD-fed and vehicle-treated group; CD + CBZ-L, CDAHFD-fed and cabozantinib (1 mg/kg)-treated group; CD + CBZ-H, CDAHFD-fed and cabozantinib (2 mg/kg)-treated group. (For interpretation of the references to colour in this figure legend, the reader is referred to the Web version of this article.)

3.2. Cabozantinib attenuates hepatic fibrosis progression in CDAHFD-fed rats

Next, we examined the impact of cabozantinib on CDAHFD-induced liver fibrosis development. In the livers of CDAHFD-fed rats, we observed extensive collagen deposition, as indicated by an increase in Sirius Red-stained lesions, and an expansion of α-smooth muscle actin^{+} myofibroblasts along with collagen deposition (Fig. 2A−2C). Notably, both doses of cabozantinib significantly attenuated the fibrotic changes (Fig. 2A−2C). In particular, treatment with cabozantinib (2 mg/kg) reduced the degree of liver fibrosis development in CDAHFD-fed rats by approximately 25 %. Consistently, the hepatic content of hydroxyproline, a major component of collagen, was reduced by cabozantinib treatment at both doses (Fig. 2D). Additionally, a significant reduction in the hepatic expressions of fibrogenic genes (*Acta2*, *Col1a1*, and *Tgfb1*) was observed in cabozantinib-treated rats (Fig. 2E).

3.3. Cabozantinib inhibits the GAS6/AXL signaling in activated HSCs

The GAS6/AXL signaling is reported to promote hepatic fibrogenesis in MASH [11]. Therefore, we investigated whether cabozantinib's antifibrotic effect is linked to its inhibition of the GAS6/AXL signaling. Fig. 3A showed that the serum levels of GAS6 were elevated in CDAHFD-fed rats, and treatment with cabozantinib further increased these levels. Additionally, CDAHFD-fed rats exhibited a higher hepatic mRNA expression of *AXL*, which was significantly reduced by cabozantinib treatment at both low and high doses (Fig. 3B). Next, the impact of cabozantinib on activated human HSCs was assessed in relation to the GAS6/AXL signaling pathway using LX-2 cells, a human HSC line. The effect of cabozantinib at the 0−50 nM range was investigated because the cytotoxicity is observed above 50 nM in LX-2 cells (Supplementary Fig. 1A in Supplementary Material). Our findings revealed that cabozantinib effectively inhibited rGAS6-induced AXL phosphorylation in LX-2 cells and attenuated Akt phosphorylation in a dose-dependent manner along with AXL phosphorylation (Fig. 3C). Consequently, cabozantinib significantly reduced the proliferative capacity of rGAS6-stimulated LX-2 cells (Fig. 3D). Moreover, stimulation with rGAS6 augmented the profibrogenic activity in a time dependent manner, as indicated by an upregulation of fibrogenic gene expressions in LX-2 cells (Fig. 3E). Notably, cabozantinib dose-dependently inhibited the upregulation of these genes (Fig. 3F).

3.4. Cabozantinib suppresses hepatic macrophage activation in CDAHFD-fed rats

Our results revealed that treatment with cabozantinib reduced hepatic inflammation scores without improving steatosis and ballooning in the CDAHFD-fed rats (Fig. 1E−H). Therefore, we hypothesized that cabozantinib might affect macrophages as well as activated HSCs. In the CDAHFD-fed rats, CD68-positive macrophages infiltrated the liver extensively, and cabozantinib significantly reduced macrophage infiltration at both 1 mg/kg and 2 mg/kg doses (Fig. 4A and B). Consistent with reduced macrophage infiltration, cabozantinib-treated rats exhibited a profound decrease in hepatic gene expressions of inflammatory cytokines (Fig. 4C). Furthermore, CDAHFD-fed rats exhibited an increase in hepatic mRNA levels of LPS-binding protein, a hepatogenic glycoprotein binding to LPS and augmenting the body's immune response. However, cabozantinib treatment did not alter LPS-binding protein expression (Fig. 4D). Therefore, the impact of cabozantinib on the inflammatory response to LPS was assessed in THP-1 cells, a human macrophage. The study was performed by adding cabozantinib at a concentration that was not cytotoxic to THP-1 cells (0−50 nM) (Supplementary Fig. 1B in Supplementary Material). As shown in Fig. 4E, LPS challenge increased the mRNA expression of inflammatory cytokines. These proinflammatory changes were significantly suppressed by cabozantinib treatment (Fig. 4E).

3.5. Cabozantinib inhibits VEGF-mediated HSC activation and intrahepatic angiogenesis in CDAHFD-fed rats

Cabozantinib is known to inhibit VEGFR2. CDAHFD-fed rats showed a marked increase in hepatic VEGFA content compared to CSANFD-fed control rats (Fig. 5A). Consistently, hepatic gene expressions of *Vegfa* and *Vegfr2* were upregulated in CDAHFD-fed rats in line with hepatic fibrosis development (Fig. 5B and C). Treatment with cabozantinib significantly reduced VEGFA content and mRNA expression of *Vegfa* and *Vegfr2* (Fig. 5A−5C). Our previous report demonstrated that VEGFA can promote collagen synthesis and proliferation in activated HSCs (18). Accordingly, the impact of cabozantinib on VEGFA-stimulated LX-2 cells was investigated. It was found that *Col1a1* mRNA expression was increased in LX-2 cells cultured with VEGFA (Fig. 5D). Notably, cabozantinib suppressed the VEGFA-induced upregulation of Col1a1 at 10 and 50 nM (Fig. 5D). Additionally, VEGFA stimulation enhanced the proliferative activity of LX-2 cells, which was attenuated by treatment with cabozantinib at 50 nM (Fig. 5E).

The impact of cabozantinib on proangiogenic activity in the livers of CDAHFD-fed rats was demonstrated by a decrease in hepatic VEGFA content and *Vegfa/Vegfr2* mRNA expression. Indeed, CD34-positive intrahepatic neovascularization was significantly reduced by administration of cabozantinib in CDAHFD-fed rats (Fig. 5F and G). Additionally, the hepatic expression of other angiogenic markers, including von Willebrand factor (*Vwf*) and angiopoietin-2 (*Ang2*) was downregulated in the cabozantinib-treated CDAHFD-fed rats (Fig. 5H). These findings indicate that cabozantinib suppresses intrahepatic angiogenesis in the CDAHFD-fed MASH fibrosis model. To further support this concept, we assessed the impact of cabozantinib on VEGFA-stimulated vascular endothelial cells. Cabozantinib at the concentrations of 0–50 nM, which did not have the cytotoxicity, effectively suppressed the VEGFA-stimulated proliferation of HUEhT-1 cells, a human umbilical vascular endothelial cell line (Supplementary Fig. 1C in Supplementary Material and Fig. 5I).

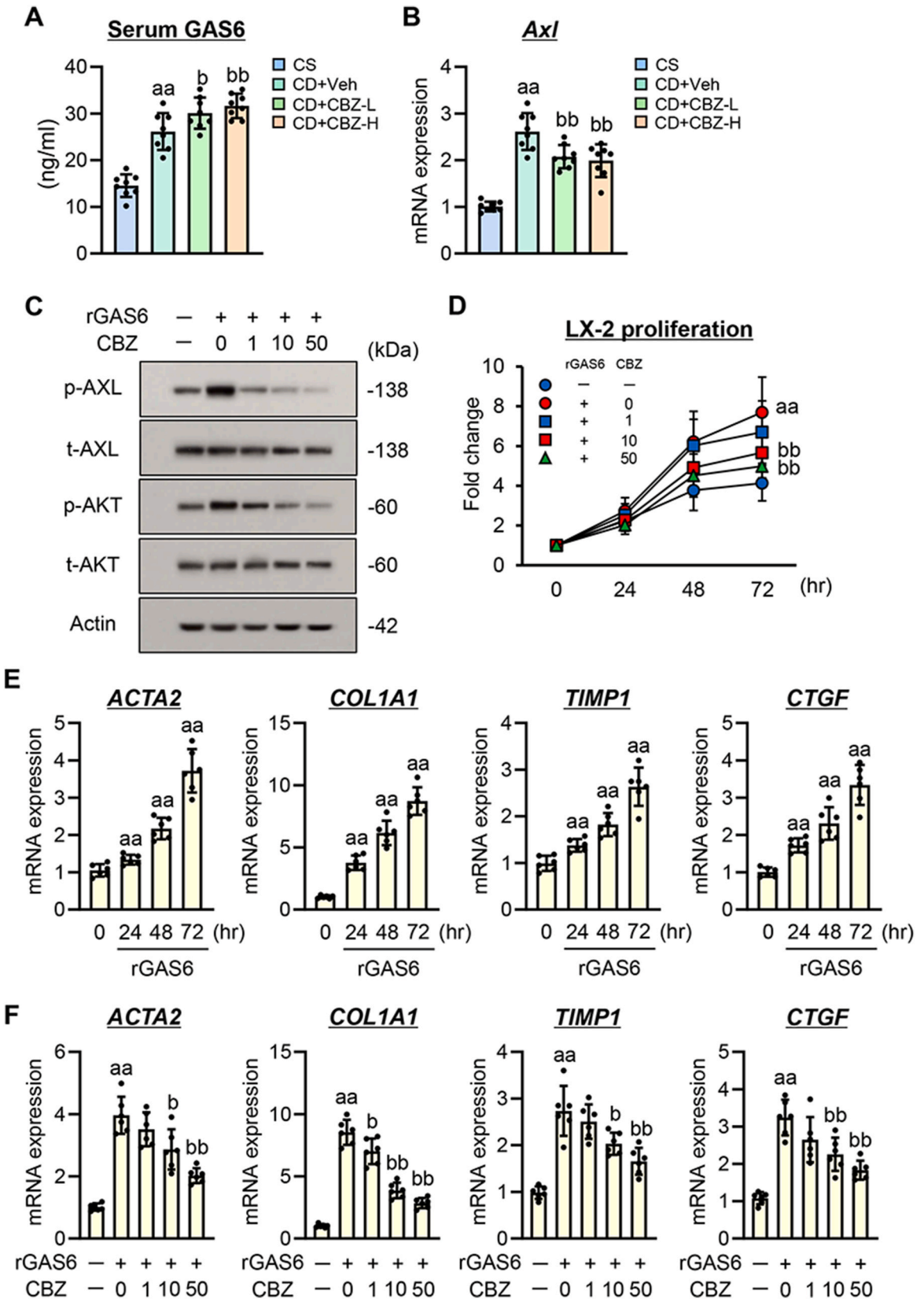

(caption on next page)

Fig. 3. Effect of cabozantinib on GAS6/AXL signaling in LX-2 cells. (A) Serum Gas6 level in the experimental rats. (B) Hepatic mRNA expression of Axl in the experimental rats. (C) Western blotting for the effect of cabozantinib (CBZ) (0−50 nM) on the phosphorylation of AXL and AKT in rGAS6 (500 ng/mL)-stimulated LX-2 cells. Whole images of blotting were shown in Supplementary Fig. 2 in Supplementary Material. (D) Effect of CBZ (0−50 nM) on rGAS6 (500 ng/mL)-induced LX-2 proliferation. (E) Inducible effect of rGAS6 (500 ng/mL) on the mRNA expression of profibrogenic markers (ACTA2, COL1A1, TIMP1 and CTGF) in LX-2 cells. (F) Effect of CBZ (0−50 nM) on the mRNA expression of profibrogenic markers in rGAS6 (500 ng/mL)-stimulated LX-2 cells. Gapdh/GAPDH was used as an internal control for qRT-PCR (B, E and F). Actin was used as an internal control for western blotting (C). Quantitative values are indicated as fold changes to the values of CS group (B), the value of each group at 0 h (D), the value at 0 h (E) and the value of rGAS6 (−)/CBZ (−) group (F). Data are the mean ± SD (n = 8; A and B, n = 6; D−F). [a, aa]: $P < 0.05$, 0.01 vs CS group (A and B), rGAS6 (−)/CBZ (−) group at 72 h (D), 0 h group (E), rGAS6 (−)/CBZ (−) group (F), [b, bb]: $P < 0.05$, 0.01 vs CD + Veh group (A and B), rGAS6 (+)/CBZ (−) group at 72 h (D), rGAS6 (+)/CBZ (−) group (F) significant difference between groups by Student's t-test. CS, CSANFD-fed and vehicle-treated group; CD + Veh, CDAHFD-fed and vehicle-treated group; CD + CBZ-L, CDAHFD-fed and cabozantinib (1 mg/kg)-treated group; CD + CBZ-H, CDAHFD-fed and cabozantinib (2 mg/kg)-treated group.

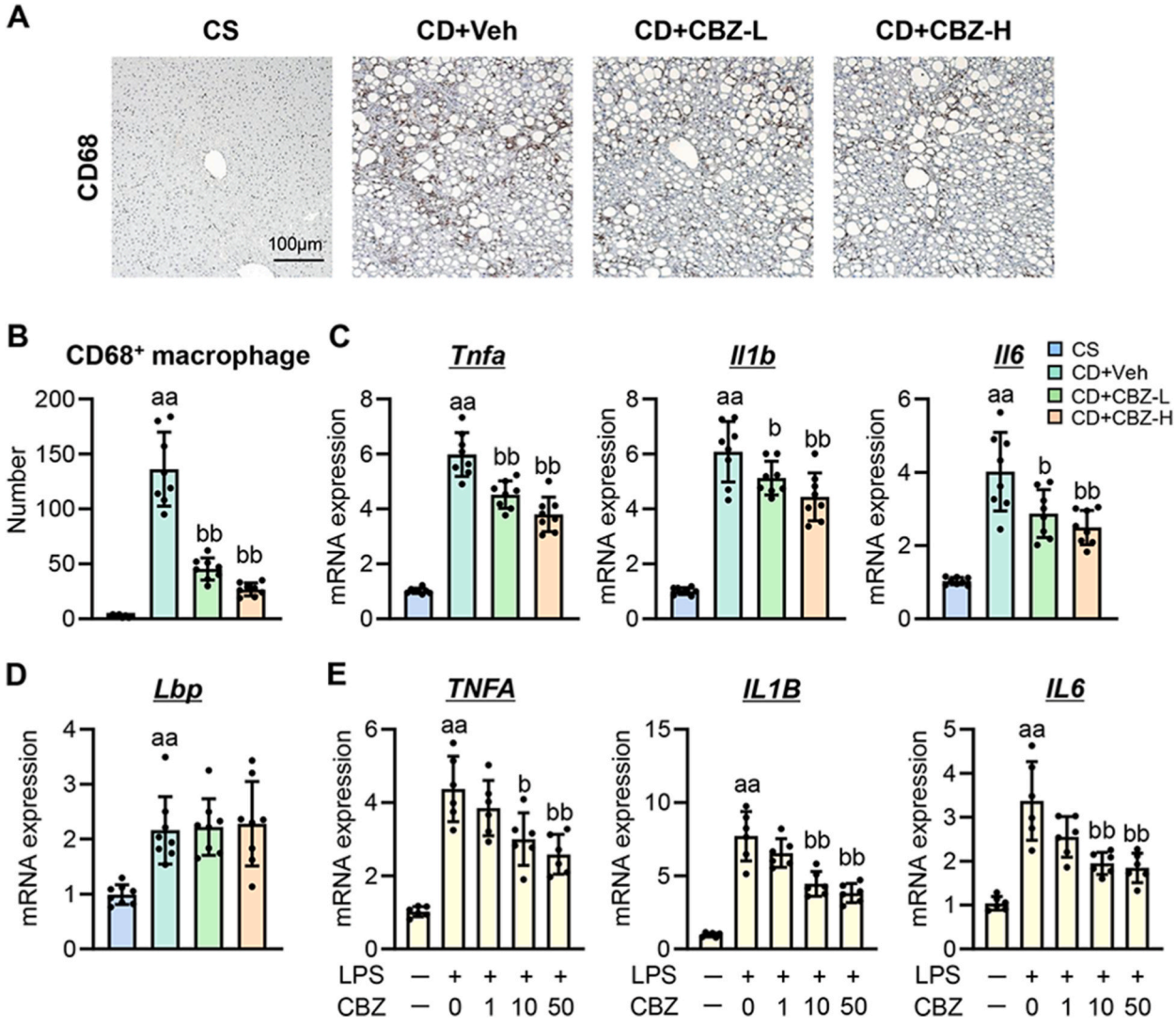

Fig. 4. Effect of cabozantinib on macrophage activation in CDAHFD-fed rats and THP cells. (A) Representative microphotographs of CD68 staining of the livers in the experimental rats. (B) Quantification of CD68-positive macrophage in high-power field. (C) Hepatic mRNA expression of proinflammatory cytokines (Tnfa, Il1b and Il6) in the experimental rats. (D) Hepatic mRNA expression of Lbp in the experimental rats. (E) Effect of cabozantinib (CBZ) (0−50 nM) on the mRNA expression of proinflammatory cytokines in LPS (50 ng/mL)-stimulated THP-1 cells. Gapdh/GAPDH was used as an internal control for qRT-PCR (C–E). Quantitative values are indicated as fold changes to the values of CS group (C and D), and the value of LPS (−)/CBZ (−) group (E). Data are the mean ± SD (n = 8; B−D, n = 6; E). [a, aa]: $P < 0.05$, 0.01 vs CS group (B–D), LPS (−)/CBZ (−) group (E), [b, bb]: $P < 0.05$, 0.01 vs CD + Veh group (B–D), and LPS (+)/CBZ (−) group (E) significant difference between groups by Student's t-test. CS, CSANFD-fed and vehicle-treated group; CD + Veh, CDAHFD-fed and vehicle-treated group; CD + CBZ-L, CDAHFD-fed and cabozantinib (1 mg/kg)-treated group; CD + CBZ-H, CDAHFD-fed and cabozantinib (2 mg/kg)-treated group.

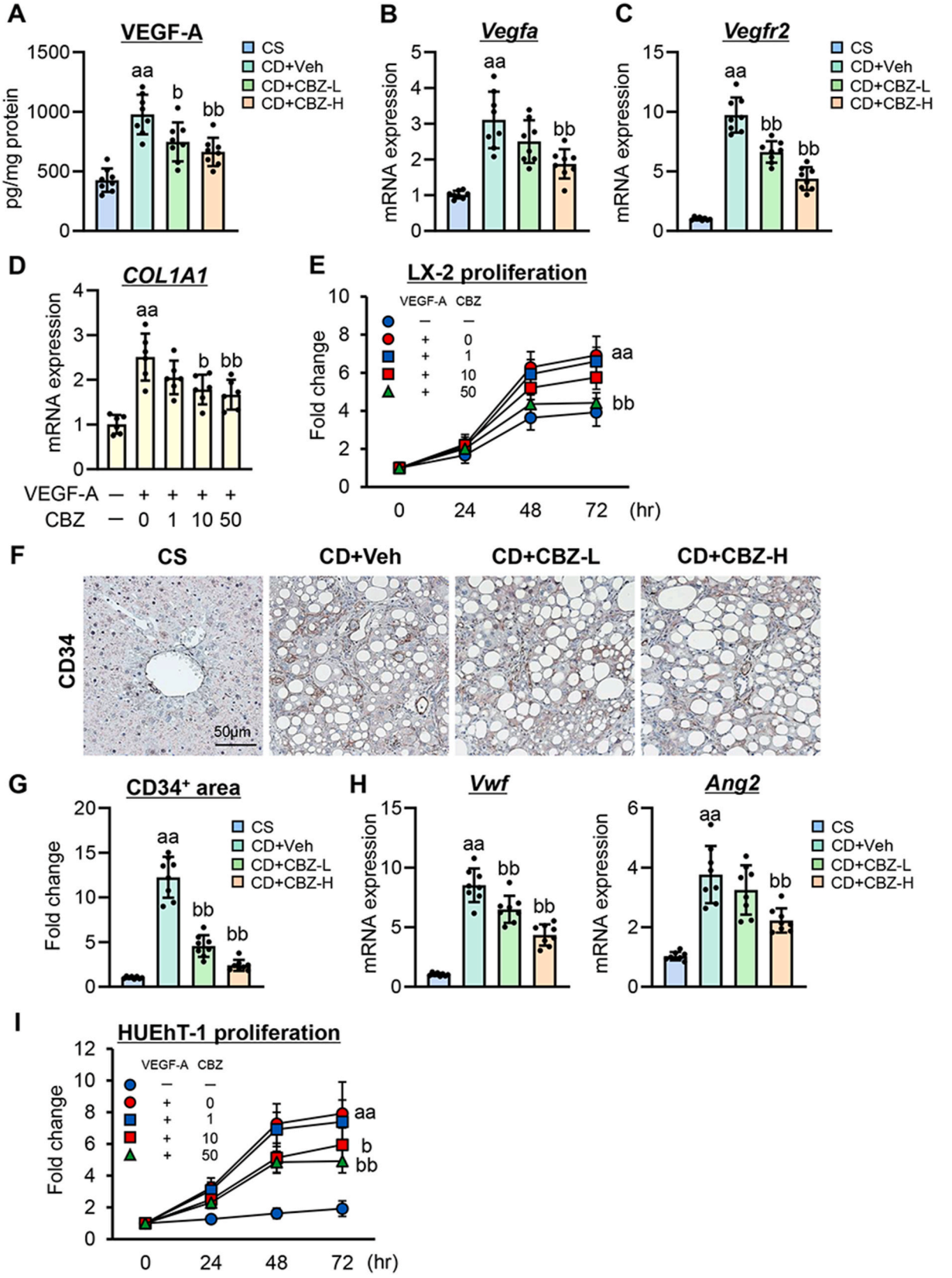

(caption on next page)

Fig. 5. Effect of cabozantinib on pathological angiogenesis and VEGF signaling in LX-2 and HUEhT-1 cells. (A) Hepatic VEGF-A content in the experimental rats. (B and C) Hepatic mRNA expression of (B) Vegfa and (C) Vegfr2 in the experimental rats. (D and E) Effect of cabozantinib (CBZ) (0−50 nM) on (D) COL1A1 expression and (E) proliferation in VEGF-A (10 ng/mL)-stimulated LX-2 cells. (F) Representative microphotographs of CD34 staining of the livers in the experimental rats. (G) Quantification of CD34-positive neovascularization in high-power field. (H) Hepatic mRNA expression of Vwf and Ang2 in the experimental rats. (I) Effect of CBZ (0−50 nM) on cell proliferation in VEGF-A (10 ng/mL)-stimulated HUEhT-1 cells. Gapdh/GAPDH was used as an internal control for qRT-PCR (B−D and H). Quantitative values are indicated as fold changes to the values of CS group (B, C, G and H), and the value of VEGF-A (−)/CBZ (−) group (D), the value of each group at 0 h (E and I). Data are the mean ± SD (n = 8; A−C, G and H, n = 6; D, E and I). [a, aa]: $P < 0.05$, 0.01 vs CS group (A−C, G and H), VEGF-A (−)/CBZ (−) group (D), VEGF-A (−)/CBZ (−) group at 72 h (E and I), [b, bb]: $P < 0.05$, 0.01 vs CD + Veh group (A−C, G and H), and VEGF-A (+)/CBZ (−) group (D), VEGF-A (+)/CBZ (−) group at 72 h (E and I), significant difference between groups by Student's t-test. CS, CSANFD-fed and vehicle-treated group; CD + Veh, CDAHFD-fed and vehicle-treated group; CD + CBZ-L, CDAHFD-fed and cabozantinib (1 mg/kg)-treated group; CD + CBZ-H, CDAHFD-fed and cabozantinib (2 mg/kg)-treated group.

3.6. Cabozantinib treatment has no detrimental effect on hepatocyte proliferation and prevents hepatocarcinogenesis in CDAHFD-fed rats

Cabozantinib inhibits c-MET, which may interfere with liver regeneration during severe hepatic injury. In the CDAHFD-fed rats, proliferating hepatocytes, indicated by Ki67 positivity, were extensively observed, reflecting liver regeneration (Fig. 6A). Meanwhile, the numbers of Ki67-positive proliferative hepatocytes were not altered in the cabozantinib-treated group compared to the vehicle-treated group (Fig. 6A and B). Additionally, treatment with cabozantinib did not affect serum albumin levels in the CDAHFD-fed rats (Fig. 6C), indicating no detrimental effect on hepatocyte proliferation in the MASH fibrosis model.

Finally, the impact of cabozantinib on MASH-based hepatocarcinogenesis was assessed. To induce hepatocarcinogenesis based on MASH, rats were fed CDAHFD for 16 weeks (Fig. 6D). Progressive hepatocarcinogenesis, as indicated by an increase in the number and size of GST-P^+ preneoplastic lesions, was evident in rats fed the CDAHFD for 16 weeks (Fig. 6E−6G). Notably, treatment with cabozantinib effectively ameliorated the progression of both number and size of GST-P^+ lesions (Fig. 6E−6G).

4. Discussion

Despite the high prevalence of MASH and the associated risk of progression to cirrhosis and HCC, approved pharmacological compounds for MASH are still limited. To the best of our knowledge, we first demonstrate that cabozantinib can prevent the development of liver fibrosis and hepatocarcinogenesis in MASH. The CDAHFD-fed rats were employed as models of MASH-based liver fibrosis and hepatocarcinogenesis. The CDAHFD induces steatohepatitis with lipid metabolism failure, leading to progressive fibrosis and HCC in rodents [26,27]. In this study and another study, adult male rats were fed the CDAHFD diet for 8–9 weeks, successfully inducing steatohepatitis with advanced liver fibrosis [26,27]. A previous report suggests that 24 weeks of CDAHFD feeding would already have led to tumorigenesis, so 16 weeks of feeding was considered appropriate to evaluate preneoplastic lesions preceding tumorigenesis [28].

4.1. Inhibition of GAS6/AXL signaling on HSCs activation

Our research findings indicate that cabozantinib can attenuate hepatic fibrosis and inflammation without affecting hepatic steatosis and ballooning. Hence, the focus of our study was on the pharmacological action of cabozantinib on activated HSCs and macrophages by targeting the GAS6/AXL signaling pathway. GAS6 has been shown to have an antiapoptotic effect on HSCs and myofibroblasts, acting as a survival factor and supporting transient myofibroblast accumulation during liver healing [15]. Additionally, GAS6 produced by HSCs and infiltrating macrophages activates the AXL-mediated PI3K/Akt signaling pathway during carbon tetrachloride-induced liver injury [15]. Inhibition of the GAS6/AXL signaling pathway, either genetically or pharmacologically, can reduce HSC activation (16). In our study, serum GAS6 and hepatic AXL expression were increased in CDAHFD-fed rats. However, treatment with cabozantinib reduced hepatic AXL expression while increasing serum GAS6 levels, possibly as a compensatory mechanism. Cell-based assays demonstrated that cabozantinib effectively inhibited Akt and AXL phosphorylation induced by rGAS6 stimulation, leading to reduced cell proliferation and profibrogenic activity. These findings indicate that cabozantinib can effectively inhibit HSC activation by blocking the GAS6/AXL signaling.

4.2. Inhibition of GAS6/AXL signaling in macrophage activation

In our study, cabozantinib attenuated the infiltration of Kupffer cells and hepatic inflammation in CDAHFD-fed rats. The GAS6/AXL signaling is implicated in monocyte-macrophage activation and the inflammatory response in chronic liver disease [11]. In cirrhotic patients, an increase in AXL-positive monocytes is correlated with disease progression [29]. Thus, AXL expression in monocytes was associated with disease severity, susceptibility to infection, the development of decompensation, and prognosis [29]. However, there are conflicting findings regarding the functional role of the GAS6/AXL signaling in macrophages and the inflammatory response. Han et al. have shown that AXL deficiency can exacerbate LPS or acute carbon tetrachloride-induced inflammatory response in the liver [30]. On the other hand, Tutusaus et al. have demonstrated that GAS6-induced AXL activation in primary mouse Kupffer cells can potentiate the LPS-induced upregulation of interleukin-1 beta and interleukin-6, which have been reduced by pharmacological inhibition of AXL in Kupffer cells [11]. Our *in vitro* results also demonstrated that cabozantinib could attenuate the increase in

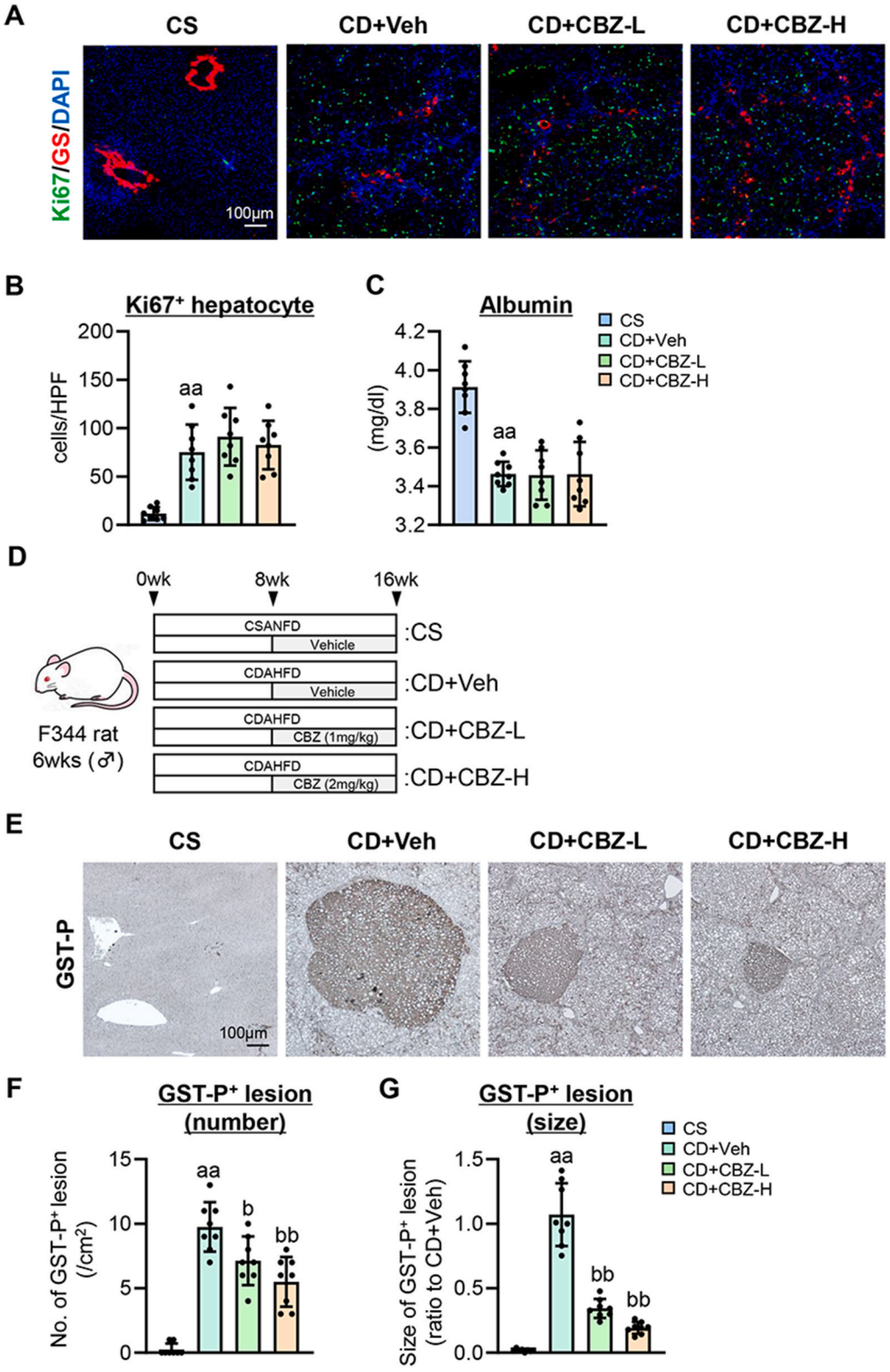

Fig. 6. Effect of cabozantinib on hepatic regeneration and hepatocarcinogenesis in CDAHFD-fed rats. (A) Representative microphotographs of double-immunofluorescence with GS/Ki67/DAPI staining in the CDAHFD-fed fibrosis model. (B) Quantitation of Ki67-positive hepatocytes in high-power field (HPF). (C) Serum albumin level in the CDAHFD-fed fibrosis model. (D) Experimental design of CDAHFD-induced hepatocarcinogenesis. (E) Representative microphotographs of placental glutathione transferase (GST-P)-positive preneoplastic foci in the experimental

rats. (F) Number of GST-P-positive neoplastic lesions per square centimeter. (G) Relative size of GST-P-positive neoplastic lesions. Data are the mean ± SD (n = 8; B, C, F and G). Quantitative values are indicated as fold changes to the values of CD + Veh group (G). [a, aa]: P < 0.05, 0.01 vs CS group, [b, bb]: P < 0.05, 0.01 vs CD + Veh group (B, C, F and G), significant difference between groups by Student's t-test. CS, CSANFD-fed and vehicle-treated group; CD + Veh, CDAHFD-fed and vehicle-treated group; CD + CBZ-L, CDAHFD-fed and cabozantinib (1 mg/kg)-treated group; CD + CBZ-H, CDAHFD-fed and cabozantinib (2 mg/kg)-treated group.

proinflammatory cytokine expression in LPS-exposed human macrophages, suggesting that cabozantinib-mediated GAS6/AXL inhibition may contribute to its antiinflammatory effects in MASH.

4.3. Inhibition of VEGF signaling in HSCs and intrahepatic angiogenesis

In addition to GAS6/AXL signaling, cabozantinib also inhibits VEGF signaling [23,24,31]. VEGF is a key angiogenic factor in chronic liver injury, promoting HSC collagen production, proliferation, and migration [17,18,32]. CDAHFD-fed rats exhibited an increase in hepatic VEGFA levels and an upregulation of VEGFA/VEGFR2 expression as liver fibrosis progressed, consistent with previous research [33]. Furthermore, VEGFA was found to stimulate collagen production and proliferation in LX-2 cells. Interestingly, cabozantinib reduced hepatic VEGFA levels and expression in rats, as well as VEGFA-induced profibrogenic effects in LX-2 cells. Blocking VEGF and various TKIs targeting VEGFR, such as brivanib and lenvatinib, can ameliorate hepatic fibrosis by suppressing HSC activation in experimental mice [21,34]. These findings suggest that cabozantinb may suppress liver fibrosis by regulating VEGF signaling in HSCs.

Moreover, we found that cabozantinib treatment suppressed intrahepatic angiogenesis by inhibiting VEGF signaling in CDAHFD-fed rats. Angiogenesis is a crucial step in inflammation and fibrosis in MASLD. Hepatic steatosis leads to hypoxia due to increased oxygen consumption from lipid metabolism and mechanical pressure on the sinusoids. Consequently, HSCs and macrophages secrete VEGF to promote angiogenesis under hypoxic conditions [35]. Indeed, patients with MASLD, especially those with advanced fibrosis, exhibited higher expression of the endothelial marker vWF in the liver [36,37]. Furthermore, patients with MASLD and advanced fibrosis have significantly elevated serum and hepatic levels of Ang2, a key factor supporting angiogenesis in pathological conditions [38]. Besides liver fibrosis development, pathological angiogenesis promotes hepatocarcinogenesis in MASH. During tumorigenesis, angiogenesis begins early, even if the tumor cells are only a few hundred cells in number [39]. Our previous report has shown a significant increase in intrahepatic neovascularization and VEGF expression during hepatocarcinogenesis in experimental MASH [40]. Therefore, cabozantinib-mediated inhibition of VEGF signaling may significantly impede liver fibrosis development and prevent hepatocarcinogenesis in MASH.

4.4. Limited impact of c-MET inhibition on liver regeneration

While cabozantinib may benefit MASH by inhibiting AXL and VEGFR, there is also a risk of detrimental consequences due to c-MET inhibition. The activation of the c-MET pathway by its ligand, hepatocyte growth factor (HGF), is known to alleviate hepatic steatosis by promoting the breakdown of accumulated lipids in MASH through the activation of fatty acid oxidation [41,42]. HGF also alleviates

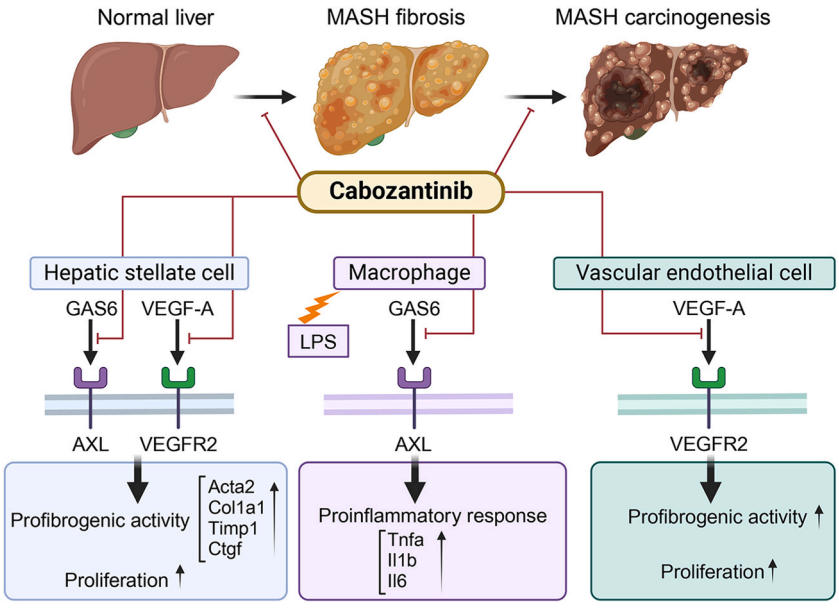

Fig. 7. Graphic representation of the effect of cabozantinib on MASH-related liver fibrosis and hepatocarcinogenesis.

inflammation caused by high-fat diet intake by suppressing the expression of inflammatory cytokines [43]. These findings suggest that the inhibition of HGF/c-MET signaling may exacerbate hepatic steatosis and inflammation, but this was not observed in our study with cabozantinib treatment. Furthermore, the HGF/c-MET signaling participates in liver regeneration, and inhibiting c-MET may delay regeneration during liver injury, including MASH [44–46]. Unexpectedly, our findings showed no obvious attenuation in hepatocyte proliferation or decline in serum albumin levels with cabozantinib treatment, indicating that the drug shows no detrimental effects in liver regeneration. Therefore, in our model, the c-MET inhibitory effect of cabozantinib appears to be limited. Further investigation into the underlying mechanism is warranted to fully understand these observations.

Despite the contributions of this study, several limitations should be acknowledged. Our data showed that cabozantinib halted the hepatic fibrosis progression in MASH alongside CDAHFD feeding. However, the effect of treatment from a condition in which liver fibrosis has already developed has not been examined. In clinical practice, it is necessary to study the efficacy of cabozantinib since it is expected to be administered to patients with advanced hepatic fibrosis. Second, the current study examined the effects of cabozantinib in only one animal model, and its effects on other MASH models need to be confirmed.

5. Conclusion

Collectively, cabozantinib demonstrated potent preventive effects on hepatic fibrosis and hepatocarcinogenesis in CDAHFD-fed rats with steatohepatitis. The underlying mechanism involves the suppression of HSC proliferation and profibrogenic activity, macrophage activation, and pathological angiogenesis *via* the inhibition of AXL and VEGFR signaling pathways (Fig. 7). Notably, cabozantinib demonstrated efficacy at a lower dose than typically used for cancer treatment without inducing hepatotoxicity in rats. Overall, these findings indicate that cabozantinib may be a therapeutic option for preventing the progression of MASH in clinical practice.

Ethical statement

All animal procedures complied with the recommendations of the Guide for Care and Use of Laboratory Animals (National Research Council of Japan), and the study was approved by the ethics committee of Nara Medical University, Kashihara, Japan (Authorization No. 13119).

Funding

This research did not receive any specific grant from funding agencies in the public, commercial, or not-for-profit sectors.

Data availability statement

Data associated with the study has not been deposited into a publicly available repository and data will be made available on request.

CRediT authorship contribution statement

Takuya Matsuda: Writing – original draft, Methodology, Investigation, Formal analysis, Data curation. **Kosuke Kaji:** Writing – review & editing, Visualization, Validation, Supervision, Resources, Methodology, Data curation, Conceptualization. **Norihisa Nishimura:** Writing – review & editing, Investigation, Formal analysis. **Shohei Asada:** Writing – review & editing, Investigation. **Aritoshi Koizumi:** Writing – review & editing, Investigation. **Misako Tanaka:** Writing – review & editing, Investigation. **Nobuyuki Yorioka:** Writing – review & editing, Investigation. **Yuki Tsuji:** Writing – review & editing, Investigation. **Koh Kitagawa:** Writing – review & editing, Visualization, Formal analysis. **Shinya Sato:** Writing – review & editing, Software. **Tadashi Namisaki:** Writing – review & editing, Methodology. **Takemi Akahane:** Writing – review & editing, Supervision. **Hitoshi Yoshiji:** Writing – review & editing, Supervision, Resources, Conceptualization.

Declaration of competing interest

The authors declare that they have no known competing financial interests or personal relationships that could have appeared to influence the work reported in this paper.

Acknowledgments

The authors would like to thank Enago (www.enago.jp) for the English language review.

Appendix A. Supplementary data

Supplementary data to this article can be found online at https://doi.org/10.1016/j.heliyon.2024.e38647.

References

[1] P. Angulo, Nonalcoholic fatty liver disease, N. Engl. J. Med. 346 (2002) 1221–1231, https://doi.org/10.1056/NEJMra011775.
[2] M.E. Rinella, J.V. Lazarus, V. Ratziu, et al., A multisociety Delphi consensus statement on new fatty liver disease nomenclature, Hepatology 78 (2023) 1966–1986, https://doi.org/10.1097/HEP.0000000000000520.
[3] M.E. Rinella, J.V. Lazarus, V. Ratziu, et al., A multisociety Delphi consensus statement on new fatty liver disease nomenclature, J. Hepatol. 79 (2023) 1542–1556, https://doi.org/10.1016/j.jhep.2023.06.003.
[4] S.L. Friedman, B.A. Neuschwander-Tetri, M. Rinella, et al., Mechanisms of NAFLD development and therapeutic strategies, Nat Med 24 (2018) 908–922, https://doi.org/10.1038/s41591-018-0104-9.
[5] T.E. Simon, B. Roelstraete, H. Khalili, et al., Mortality in biopsy-confirmed nonalcoholic fatty liver disease, Gut 70 (2021) 1375–1382, https://doi.org/10.1136/gutjnl-2020-322786.
[6] H. Hagstrom, P. Nasr, M. Ekstedt, et al., Fibrosis stage but not NASH predicts mortality and time to development of severe liver disease in biopsy-proven NAFLD, J. Hepatol. 67 (2017) 1265–1273, https://doi.org/10.1016/j.jhep.2017.07.027.
[7] S.A. Harrison, P. Bedossa, C.D. Guy, et al., A phase 3, randomized, controlled trial of resmetirom in NASH with liver fibrosis, N. Engl. J. Med. 390 (2024) 497–509, https://doi.org/10.1056/NEJMoa2309000.
[8] C. Zhu, Y. Wei, X. Wei, AXL receptor tyrosine kinase as a promising anti-cancer approach: functions, molecular mechanisms and clinical applications, Mol. Cancer 18 (2019) 153, https://doi.org/10.1186/s12943-019-1090-3.
[9] D. DeRyckere, J.M. Huelse, H.S. Earp, et al., TAM family kinases as therapeutic targets at the interface of cancer and immunity, Nat. Rev. Clin. Oncol. 20 (2023) 755–779, https://doi.org/10.1038/s41571-023-00813-7.
[10] M. Bellan, M.G. Cittone, S. Tonello, et al., Gas6/TAM system: a key modulator of the interplay between inflammation and fibrosis, Int. J. Mol. Sci. 20 (2019) 5070, https://doi.org/10.3390/ijms20205070.
[11] A. Tutusaus, E.D. Gregorio, B. Cucarull, et al., A functional role of GAS6/TAM in nonalcoholic steatohepatitis progression implicates AXL as therapeutic target, Cell Mol Gastroenterol Hepatol 9 (2020) 349–368, https://doi.org/10.1016/j.jcmgh.2019.10.010.
[12] D. Couchie, F. Lafdil, N. Martin-Garcia, et al., Expression and role of Gas6 protein and of its receptor AXL in hepatic regeneration from oval cells in the rat, Gastroenterology 129 (2005) 1633–1642, https://doi.org/10.1053/j.gastro.2005.08.004.
[13] F. Lafdil, M.N. Chobert, V. Deveaux, et al., Growth arrest-specific protein 6 deficiency impairs liver tissue repair after acute toxic hepatitis in mice, J. Hepatol. 51 (2009) 55–66, https://doi.org/10.1016/j.jhep.2009.02.030.
[14] L. Llacuna, C. Barcena, L. Bellido-Martin, et al., Growth arrest specific protein 6 is hepatoprotective against murine ischemia/reperfusion injury, Hepatology 52 (2010) 1371–1379, https://doi.org/10.1002/hep.23833.
[15] F. Lafdil, M.N. Chobert, D. Couchie, et al., Induction of Gas6 protein in CCl4- induced rat liver injury and anti-apoptotic effect on hepatic stellate cells, Hepatology 44 (2006) 228–239, https://doi.org/10.1002/hep.21237.
[16] C. Barcena, M. Stefanovic, A. Tutusaus, et al., Gas6/Axl pathway is activated in chronic liver disease and its targeting reduces fibrosis via hepatic stellate cell inactivation, J. Hepatol. 63 (2015) 670–678, https://doi.org/10.1016/j.jhep.2015.04.013.
[17] C. Bocca, E. Novo, A. Miglietta, et al., Angiogenesis and fibrogenesis in chronic liver diseases, Cell Mol Gastroenterol Hepatol 1 (2015) 477–488, https://doi.org/10.1016/j.jcmgh.2015.06.011.
[18] H. Yoshiji, S. Kuriyama, J. Yoshii, et al., Vascular endothelial growth factor and receptor interaction is a prerequisite for murine hepatic fibrogenesis, Gut 52 (2003) 1347–1354, https://doi.org/10.1136/gut.52.9.1347.
[19] M. Fernández, D. Semela, J. Bruix, et al., Angiogenesis in liver disease, J. Hepatol. 50 (2009) 604–620, https://doi.org/10.1016/j.jhep.2008.12.011.
[20] K. Qu, Z. Huang, T. Lin, et al., New insight into the anti-liver fibrosis effect of multitargeted tyrosine kinase inhibitors: from molecular target to clinical trials, Front. Pharmacol. 6 (2016) 300, https://doi.org/10.3389/fphar.2015.00300.
[21] H. Ogawa, K. Kaji, N. Nishimura, et al., Lenvatinib prevents liver fibrosis by inhibiting hepatic stellate cell activation and sinusoidal capillarization in experimental liver fibrosis, J. Cell Mol. Med. 25 (2021) 4001–4013, https://doi.org/10.1111/jcmm.16363.
[22] H. Shen, H. Yu, Q.Y. Li, et al., Hepatocyte-derived VEGFA accelerates the progression of non-alcoholic fatty liver disease to hepatocellular carcinoma via activating hepatic stellate cells, Acta Pharmacol. Sin. 43 (2022) 2917–2928, https://doi.org/10.1038/s41401-022-00907-5.
[23] F.M. Yakes, J. Chen, J. Tan, et al., Cabozantinib (XL184), a novel MET and VEGFR2 inhibitor, simultaneously suppresses metastasis, angiogenesis, and tumor growth, Mol Cancer Ther 10 (2011) 2298–2308, https://doi.org/10.1158/1535-7163.MCT-11-0264.
[24] M. Kudo, Cabozantinib as a second-line agent in advanced hepatocellular carcinoma, Liver Cancer 7 (2018) 123–133, https://doi.org/10.1159/000488542.
[25] E.M. Brunt, D.E. Kleiner, L.A. Wilson, et al., Nonalcoholic fatty liver disease (NAFLD) activity score and the histopathologic diagnosis in NAFLD: distinct clinicopathologic meanings, Hepatology 53 (2011) 810–820, https://doi.org/10.1002/hep.24127.
[26] M. Matsumoto, N. Hada, Y. Sakamaki, et al., An improved mouse model that rapidly develops fibrosis in non-alcoholic steatohepatitis, Int. J. Exp. Pathol. 94 (2013) 93–103, https://doi.org/10.1111/iep.12008.
[27] G. Wei, P. An, K.A. Vaid, et al., Comparison of murine steatohepatitis models identifies a dietary intervention with robust fibrosis, ductular reaction, and rapid progression to cirrhosis and cancer, Am. J. Physiol. Gastrointest. Liver Physiol. 318 (2020) G174–G188, https://doi.org/10.1152/ajpgi.00041.2019.
[28] A. Ikawa-Yoshida, S. Matsuo, A. Kato, et al., Hepatocellular carcinoma in a mouse model fed a choline-deficient, L-amino acid-defined, high-fat diet, Int. J. Exp. Pathol. 98 (2017) 221–233, https://doi.org/10.1111/iep.12240.
[29] R. Brenig, O.T. Pop, E. Triantafyllou, et al., Expression of AXL receptor tyrosine kinase relates to monocyte dysfunction and severity of cirrhosis, Life Sci. Alliance 3 (2019) e201900465, https://doi.org/10.26508/lsa.201900465.
[30] J. Han, J. Bae, C.Y. Choi, et al., Autophagy induced by AXL receptor tyrosine kinase alleviates acute liver injury via inhibition of NLRP3 inflammasome activation in mice, Autophagy 12 (2016) 2326–2343, https://doi.org/10.1080/15548627.2016.1235124.
[31] S. Roy, B.K. Narang, S.K. Rastogi, et al., A novel multiple tyrosine-kinase targeted agent to explore the future perspectives of anti-angiogenic therapy for the treatment of multiple solid tumors: cabozantinib, Anti Cancer Agents Med. Chem. 15 (2015) 37–47, https://doi.org/10.2174/1871520614666140902153840.
[32] E. Novo, S. Cannito, E. Zamara, et al., Proangiogenic cytokines as hypoxia-dependent factors stimulating migration of human hepatic stellate cells, Am. J. Pathol. 170 (2007) 1942–1953, https://doi.org/10.2353/ajpath.2007.060887.
[33] Y. Aihara, H. Yoshiji, R. Noguchi, et al., Direct renin inhibitor, aliskiren, attenuates the progression of non-alcoholic steatohepatitis in the rat model, Hepatol. Res. 43 (2013) 1241–1250, https://doi.org/10.1111/hepr.12081.
[34] I. Nakamura, K. Zakharia, B.A. Banini, et al., Brivanib attenuates hepatic fibrosis in vivo and stellate cell activation in vitro by inhibition of FGF, VEGF and PDGF signaling, PLoS One 9 (2014) e92273, https://doi.org/10.1371/journal.pone.0092273.
[35] V. Ankoma-Sev, Y. Wang, Z. Dai, Hypoxic stimulation of vascular endothelial growth factor expression in activated rat hepatic stellate cells, Hepatology 31 (2000) 141–148, https://doi.org/10.1002/hep.510310122.
[36] A. Kotronen, L. Joutsi-Korhonen, K. Sevastianova, et al., Increased coagulation factor VIII, IX, XI and XII activities in non-alcoholic fatty liver disease, Liver Int. 31 (2011) 176–183, https://doi.org/10.1111/j.1478-3231.2010.02375.x.
[37] A. Tripodi, A.L. Fracanzani, M. Primignani, et al., Procoagulant imbalance in patients with non-alcoholic fatty liver disease, J. Hepatol. 61 (2014) 148–154, https://doi.org/10.1016/j.jhep.2014.03.013.
[38] S. Lefere, F. Van de Velde, A. Hoorens, et al., Angiopoietin-2 promotes pathological angiogenesis and is a therapeutic target in murine nonalcoholic fatty liver disease, Hepatology 69 (2019) 1087–1104, https://doi.org/10.1002/hep.30294.
[39] C.Y. Li, S. Shan, Q. Huang, et al., Initial stages of tumor cell-induced angiogenesis: evaluation via skin window chambers in rodent models, J Natl Cancer Inst 92 (2000) 143–147, https://doi.org/10.1093/jnci/92.2.143.
[40] H. Yoshiji, S. Kuriyama, J. Yoshii, et al., Halting the interaction between vascular endothelial growth factor and its receptors attenuates liver carcinogenesis in mice, Hepatology 39 (2004) 1517–1524, https://doi.org/10.1002/hep.20218.

[41] D.C. Kroy, F. Schumacher, P. Ramadori, et al., Hepatocyte specific deletion of c-Met leads to the development of severe non-alcoholic steatohepatitis in mice, J. Hepatol. 61 (2014) 883–890, https://doi.org/10.1016/j.jhep.2014.05.019.
[42] H.K. Drescher, F. Schumacher, T. Schenker, et al., c-Met signaling protects from nonalcoholic steatohepatitis- (NASH-) induced fibrosis in different liver cell types, Oxid. Med. Cell. Longev. 2018 (2018) 6957497, https://doi.org/10.1155/2018/6957497.
[43] N. Li, Z. Dou, J. Liu, et al., Therapeutic effect of HGF on NASH mice through HGF/c-Met and JAK2-STAT3 signalling pathway, Ann. Hepatol. 17 (2018) 501–510, https://doi.org/10.5604/01.3001.0011.7395.
[44] M. Borowiak, A.N. Garratt, T. Wüstefeld, et al., Met provides essential signals for liver regeneration, Proc Natl Acad Sci U S A 101 (2004) 10608–10613, https://doi.org/10.1073/pnas.0403412101.
[45] C.G. Huh, V.M. Factor, A. Sanchez, et al., Hepatocyte growth factor/c-met signaling pathway is required for efficient liver regeneration and repair, Proc Natl Acad Sci U S A 101 (2004) 4477–4482, https://doi.org/10.1073/pnas.0306068101.
[46] V.M. Factor, D. Seo, T. Ishikawa, et al., Loss of c-Met disrupts gene expression program required for G2/M progression during liver regeneration in mice, PLoS One 5 (2010) e12739, https://doi.org/10.1371/journal.pone.0012739.